

## Supporting Information

### Asymmetrical etching of Ag nanoparticles into symmetry-reduced bi-metallic nanocups at the single-nanoparticle level

Huan-Huan Xue,<sup>†a</sup> Wen-Jin Shen,<sup>†a</sup> Wen-Chao Geng,<sup>a</sup> Xia Yin,<sup>a</sup> Yue Yang,<sup>a</sup>  
Shaojun Guo<sup>\*b</sup> and Yong-Jun Li<sup>\*a</sup>

<sup>a</sup>State Key Lab of Chemo/Biosensing and Chemometrics, College of Chemistry and Chemical Engineering, Hunan University, Changsha 410082, China

<sup>b</sup>Department of Materials Science and Engineering, College of Engineering, Peking University, Beijing 100871, China

<sup>†</sup>These authors contributed equally.

#### Materials and Methods:

##### 1.1 Chemicals

Ethylene glycol (EG, 99%), ethanol (C<sub>2</sub>H<sub>5</sub>OH, 99.7%), acetone (99.5%), sodium citrate (99%), tannic acid (99%), copper dichloride (CuCl<sub>2</sub>, 99%), silver nitrate (AgNO<sub>3</sub>, 99.8%) and sodium borohydride (NaBH<sub>4</sub>, 96%) were supplied by Sinopharm Chemical Reagent Co. Ltd (China); 1,5-pentanediol (97%), polyvinylpyrrolidone (PVP, MW ≈ 29 000 and 55 000) and gold (III) chloride trihydrate (HAuCl<sub>4</sub>·3H<sub>2</sub>O, ≥ 49.0% Au basis) were purchased from Sigma-Aldrich; sodium sulfide (Na<sub>2</sub>S, 98%) was obtained from Tianjin Damao Chemical Reagent Co. Ltd (China). All chemical reagents were used as received except that EG was refluxed at 196 °C for 5 h to remove trace water. All solutions were prepared with Milli-Q water (18.2 MΩ·cm).

##### 1.2 Synthesis

###### 1.2.1 Silver nanocubes with average side length of ~100 nm<sup>1,2</sup>

Stock solution 1: CuCl<sub>2</sub> (7 μL, 0.047 mol/L) was added into 2 mL of 1,5-pentanediol solution containing AgNO<sub>3</sub> (0.165 mol/L).

Stock solution 2: PVP (MW = 55000, 40 mg) was dissolved into 2 mL of 1,5-pentanediol.

1,5-pentanediol (5 mL) was heated to 190 °C at reflux for 2 min, to which was added alternately two precursor solutions at different rates: 125 μL of stock solution 1 every minute and 80 μL of stock solution 2 every 30 s. After repeating this addition for eight times, the reaction was continued for 2 min and quenched by transferring the solution into an ice-cold water bath. The product was collected by centrifugation and successively washed with acetone (1 × 5 mL) and water (1 × 5 mL). The resulting Ag nanocubes with an average side length of ~100 nm (Fig. S1) were redispersed into 100 mL of ethanol for further use.

###### 1.2.2 Silver nanocubes with average side length of ~45 nm<sup>3</sup>

EG (6 mL) was added into a 25-mL three-necked flask under vigorous stirring and heated to 150 °C at argon atmosphere with a flow at 120 mL/min, to which, after 1 h, was added Na<sub>2</sub>S (70

$\mu\text{L}$ ,  $3 \text{ mmol}\cdot\text{L}^{-1}$ ) and PVP (MW  $\approx 29\,000$ ,  $1.5 \text{ mL}$ ,  $20 \text{ mg/mL}$ ) EG solution. After 8-9 min,  $0.5 \text{ mL}$  of EG containing  $\text{AgNO}_3$  ( $48 \text{ mg/mL}$ ) was added. After  $\sim 20 \text{ min}$ , the solution turned from light yellow to green-ochre, and then the reaction was quenched by transferring the solution into an ice-cold water bath. The product was collected by centrifugation and successively washed with acetone ( $1 \times 10 \text{ mL}$ ) and water ( $1 \times 10 \text{ mL}$ ). The resulting Ag nanocubes with an average side length of  $\sim 45 \text{ nm}$  (Fig. S10a) were redispersed into  $100 \text{ mL}$  of ethanol for later use.

### *1.2.3 Silver nanowires<sup>4</sup>*

EG ( $10 \text{ mL}$ ) was refluxed in a three-necked round-bottom flask at  $160 \text{ }^\circ\text{C}$  for  $1 \text{ h}$ , to which were added two EG solutions at the same rate of  $0.2 \text{ mL}\cdot\text{min}^{-1}$  under vigorous stirring:  $\text{AgNO}_3$  ( $5 \text{ mL}$ ,  $0.2 \text{ mol}\cdot\text{L}^{-1}$ ) and PVP (MW  $\approx 29\,000$ ) ( $5 \text{ mL}$ ,  $0.3 \text{ mol}\cdot\text{L}^{-1}$ ). After  $\sim 45 \text{ min}$ , the solution color turned to opaque gray, indicative of the formation of silver nanowires. The resulting product was collected by centrifugation, successively washed with acetone ( $1 \times 10 \text{ mL}$ ) and water ( $1 \times 10 \text{ mL}$ ), and redispersed in  $250 \text{ mL}$  ethanol for further use. SEM image (Fig. S10b) shows that Ag nanowires have a high aspect ratio with an average diameter of  $\sim 100 \text{ nm}$ .

### *1.2.4 Silver nanospheres<sup>5</sup>*

Aqueous solution ( $100 \text{ mL}$ ) containing sodium citrate ( $5 \text{ mmol}\cdot\text{L}^{-1}$ ) and tannic acid ( $5 \text{ mmol}\cdot\text{L}^{-1}$ ) was heated to  $100 \text{ }^\circ\text{C}$  at reflux under vigorous stirring, to which  $\text{AgNO}_3$  aqueous solution ( $1 \text{ mL}$ ,  $25 \text{ mmol}\cdot\text{L}^{-1}$ ) was added. After  $10 \text{ min}$ , the solution was cooled to room temperature. The product was collected by centrifugation, washed with water ( $2 \times 50 \text{ mL}$ ), and redispersed in  $50 \text{ mL}$  ethanol for further use. TEM image (Fig. S10c) shows that Ag nanoparticles have an average diameter of  $\sim 46 \text{ nm}$ .

## ***1.3 Assembly of Ag nanoparticles at toluene/water interface***

Assembly of Ag nanoparticle monolayer at toluene/water interface was performed according to our previous reports<sup>6</sup> with minor modification.

Ag nanoparticles colloid ( $800 \mu\text{L}$ ) and toluene ( $2 \text{ mL}$ ) were mixed in a  $10\text{-mL}$  beaker under sonication, into which was rapidly poured  $\text{H}_2\text{O}$  ( $7 \text{ mL}$ ). An toluene/water interface was formed quickly between toluene and water. Initially, the top toluene phase was extremely turbid due to the emulsification of water in toluene whereas the bottom water phase was colorless and transparent. After keeping the mixture silence for several hours, the toluene phase became colorless and clear due the phase separation of water and toluene. Meantime, a pale yellow membrane was observed between water and toluene, i.e. at the interface, indicating that Ag nanocubes have been captured by the toluene/water interface. After evaporation of toluene, Ag nanoparticle monolayer was subjected to oriented etching.

### ***1.4 Fabrication of nanocontainers by oriented etching***

To etch Ag nanocubes, nanospheres, nanowires and into Au/Ag nanocups and nanotroughs,  $\text{HAuCl}_4$  ( $10 \mu\text{L}$ ,  $25.4 \text{ mmol}\cdot\text{L}^{-1}$ ) aqueous solution, except for the etching of Ag/Au nanotroughs with  $20 \mu\text{L}$  of  $\text{HAuCl}_4$ , was injected into the water phase with a syringe, stirred gently for  $30 \text{ seconds}$  (*Tips*: do not disturb the interfacial monolayer) and kept still to complete the etching of Ag nanoparticles.

To etch ~45-nm Ag nanocubes into Pt/Ag and Pd/Ag nanocups,  $\text{H}_2\text{PtCl}_6$  (20  $\mu\text{L}$ , 20  $\text{mmol}\cdot\text{L}^{-1}$ ) or  $\text{H}_2\text{PdCl}_4$  (37  $\mu\text{L}$ , 20  $\text{mmol}\cdot\text{L}^{-1}$ ) aqueous solution was injected into the water phase with a syringe, stirred gently for 30 seconds and kept still to complete the etching of Ag nanocubes.

The etching depth as well as the compositions of the resulting nanocontainers can be tuned easily by controlling etching time.

### ***1.5 Transfer of the resulting nanocontainer monolayer***

Transfer of the resulting nanocontainer monolayer is similar to our previously reported technological process.<sup>6,7</sup> Briefly, clean substrates were used to touch and load nanocontainer monolayers from the water phase (Scheme 1d). Collected nanocontainer monolayers were characterized directly by SEM, and redispersed into ethanol or water by sonification for TEM imaging.

### ***1.6 Characterization and instrumentation***

Transmission electron microscopy (TEM) and scanning electron microscopy (SEM) images were obtained on a JEM-3010 microscope (JEOL, Japan) and a S-4800 microscope (JEOL, Japan), respectively. Elemental mapping analysis was performed in the STEM mode on a FEI Tecnai G2 F20 Field Emission TEM microscope. Visual angle-varied SEM images were obtained on FEI Helios NanoLab G3 UC dual-beam microscope. X-ray photoelectron spectroscopy (XPS) was conducted on K-Alpha 1063 X-ray photoelectron spectrometer (Thermo Fisher Scientific, UK) with Al  $\text{K}\alpha$  X-ray source. X-ray diffraction (XRD) measurement was performed on a  $\theta$ - $2\theta$  X-ray diffraction Siemens D5000 apparatus. UV-Vis spectra were measured on a UV-1800 spectrophotometer (Shimadzu Corporation, Japan).

## Supplement Figures and Text

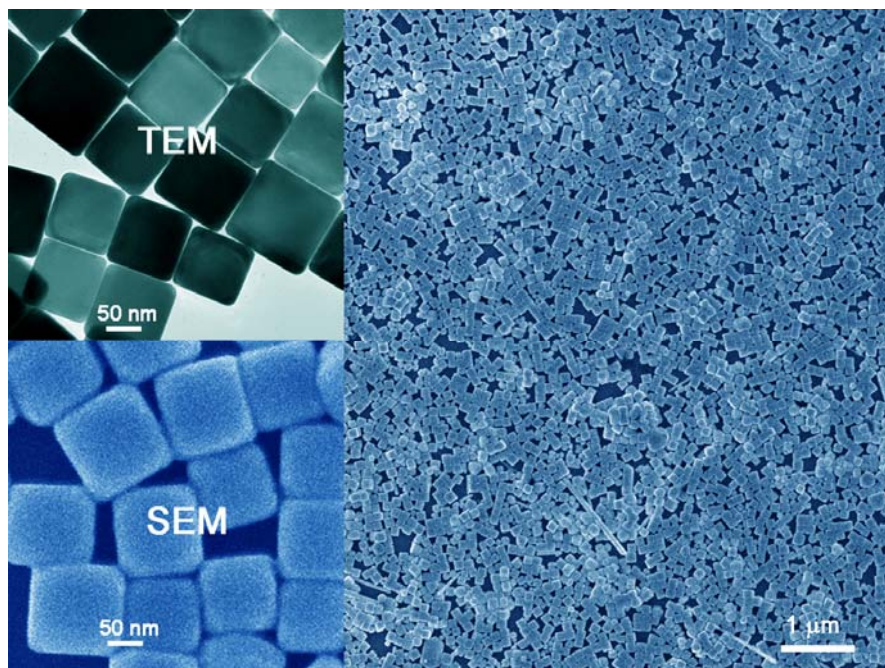


**Fig. S1** SEM image of ~100-nm Ag nanocube monolayer located at water/air interface. Inset: magnified TEM and SEM images.

(a)

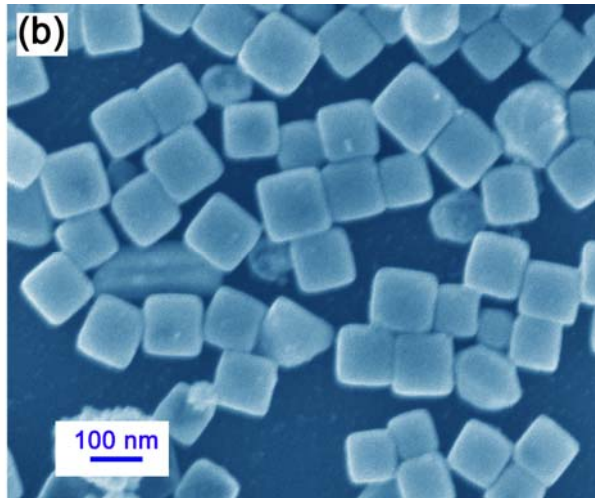
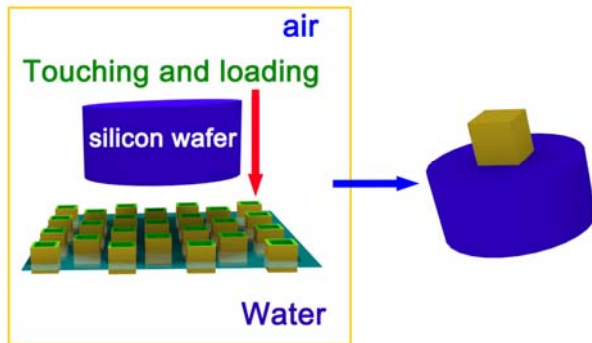


**Fig. S2** Illustration of nanoparticle monolayer transfer to substrate (e.g. silicon wafer) by “touching and loading” method from the air phase (a) and the corresponding SEM image (b).

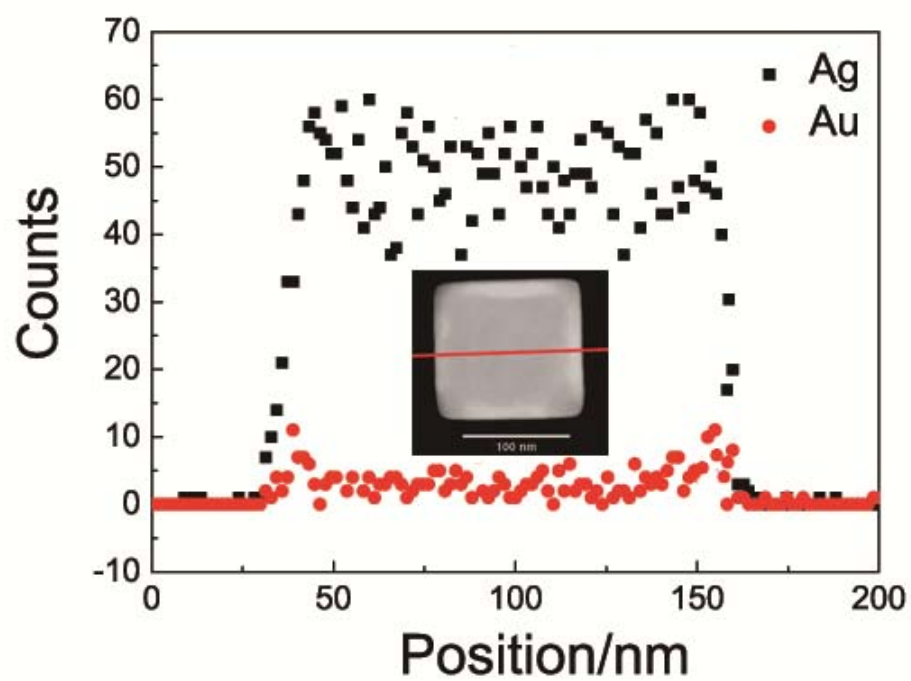


**Fig. S3** STEM-EDX linear scan element-distribution profile of Ag/Au nanocup. Inset: the corresponding STEM image.

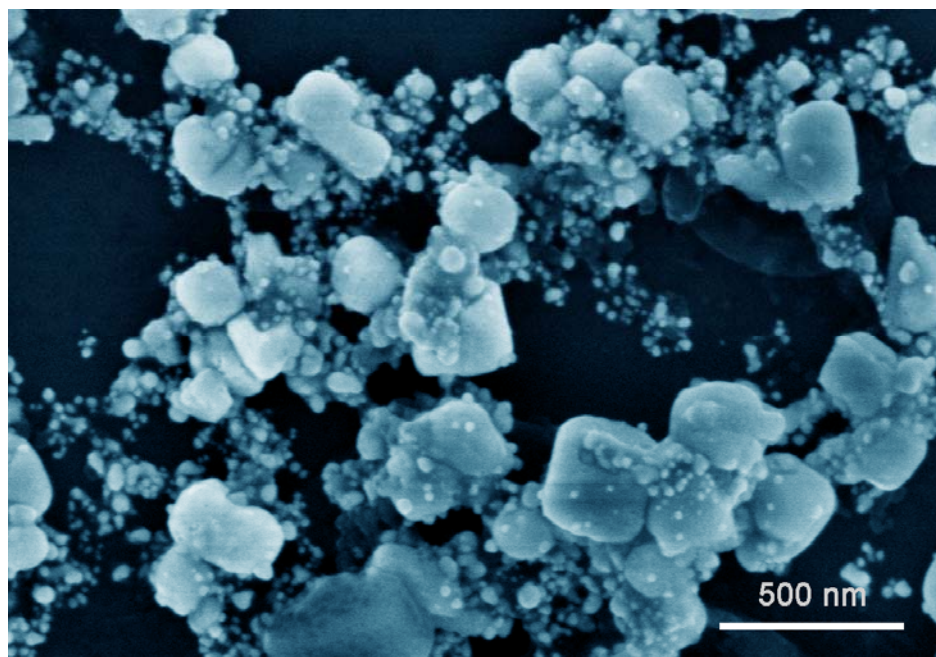


**Fig. S4** SEM image of products obtained by etching Ag nanocubes in solution with HAuCl<sub>4</sub> for 60 min.

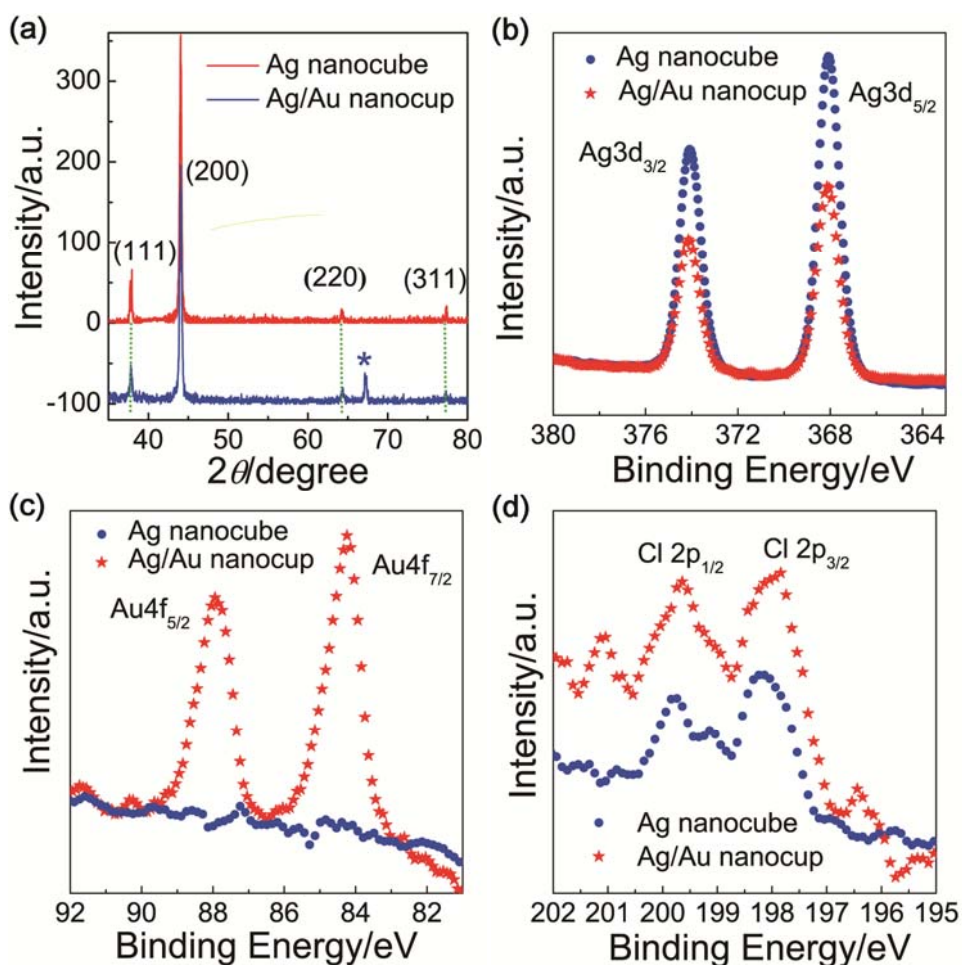


**Fig. S5** (a) XRD patterns of Ag/Au nanocups and Ag nanocubes and (b) Ag 3d (b), Au 4f (c) and Cl 2p (d) XPS spectra of Ag/Au nanocups and Ag nanocubes.

The resulting Ag/Au nanocups have a typical face-centered cubic (fcc) crystalline structure (Fig. S5a); the characteristic diffraction peaks of (111), (200), (220) and (311) facets similar to pure Ag nanocubes were observed, consistent with standard values of Ag (JCPDS PDF 65-8428). Separate contribution of Ag and Au cannot be distinguished due to the similarity of their diffraction peak positions. The relative intensity ratio of (200) to (111) peaks is much larger than 1, implying that Au/Ag nanocups are still enclosed with abundant (100) facets,<sup>8</sup> similar to pure Ag nanocubes. Additionally, A new peak at  $\sim 67.19^\circ$  (marked with \*) was attributed to the diffraction of (400) facets of side products, i.e. AgCl (JCPDS PDF 31-1238). XPS spectra of Ag/Au nanocups (Fig. S5b and c) show well-defined binding energy bands of Ag 3d<sub>3/2</sub> and 3d<sub>5/2</sub>



(~374.05 and ~368.05 eV, respectively), and Au  $4f_{5/2}$  and  $4f_{7/2}$  (~88.14 and 84.44 eV, respectively) whereas Au species cannot be detected in pure Ag nanocubes (Fig. S5c). Moreover, each binding energy band of Ag and Au is symmetrical, and the differences between the  $4f_{7/2}$  and  $4f_{5/2}$  peaks for gold (3.65 eV) as well as between the  $3d_{5/2}$  and  $3d_{3/2}$  peaks for silver (6.0 eV) are also exactly the same as the standard values of  $Ag^0$  and  $Au^0$ ,<sup>9</sup> implying that  $Ag^0$  and  $Au^0$  dominate the final nanocups. The characteristic binding energy of  $Cl^-$  ions was also detected in Ag/Au nanocups (Fig. S5d) ( $Cl\ 2p_{1/2}$ , ~199.5 eV;  $Cl\ 2p_{3/2}$ , ~199.5 eV), the abundance of which is almost identical to that of Ag nanocubes, suggesting that AgCl adhering to Ag/Au nanocups is negligible.

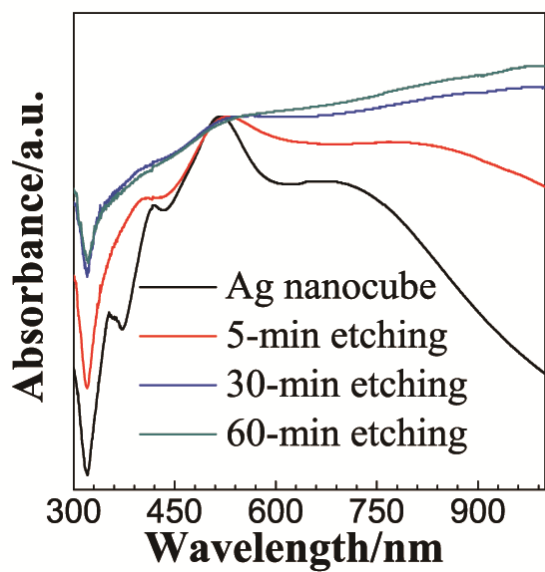


**Fig. S6** UV-vis spectra of Ag nanocubes and the products obtained by different etching time with  $\text{AuCl}_4^-$ .

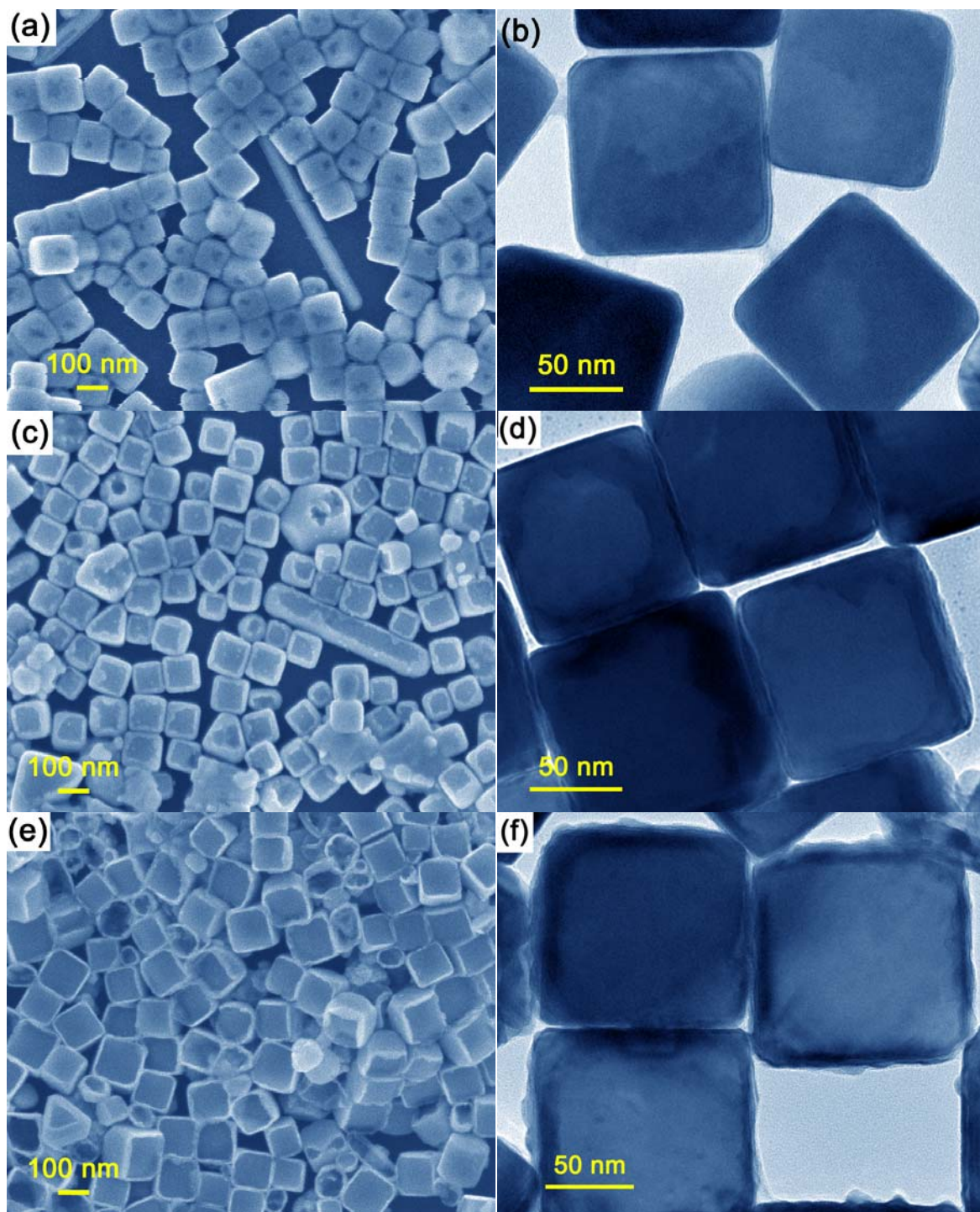


**Fig. S7** SEM (a, c and e) and TEM (b, d and f) images of Ag/Au nanocups obtained by etching for different time: 5 min (a and b), 30 min (c and d), and 90 min (e and f).

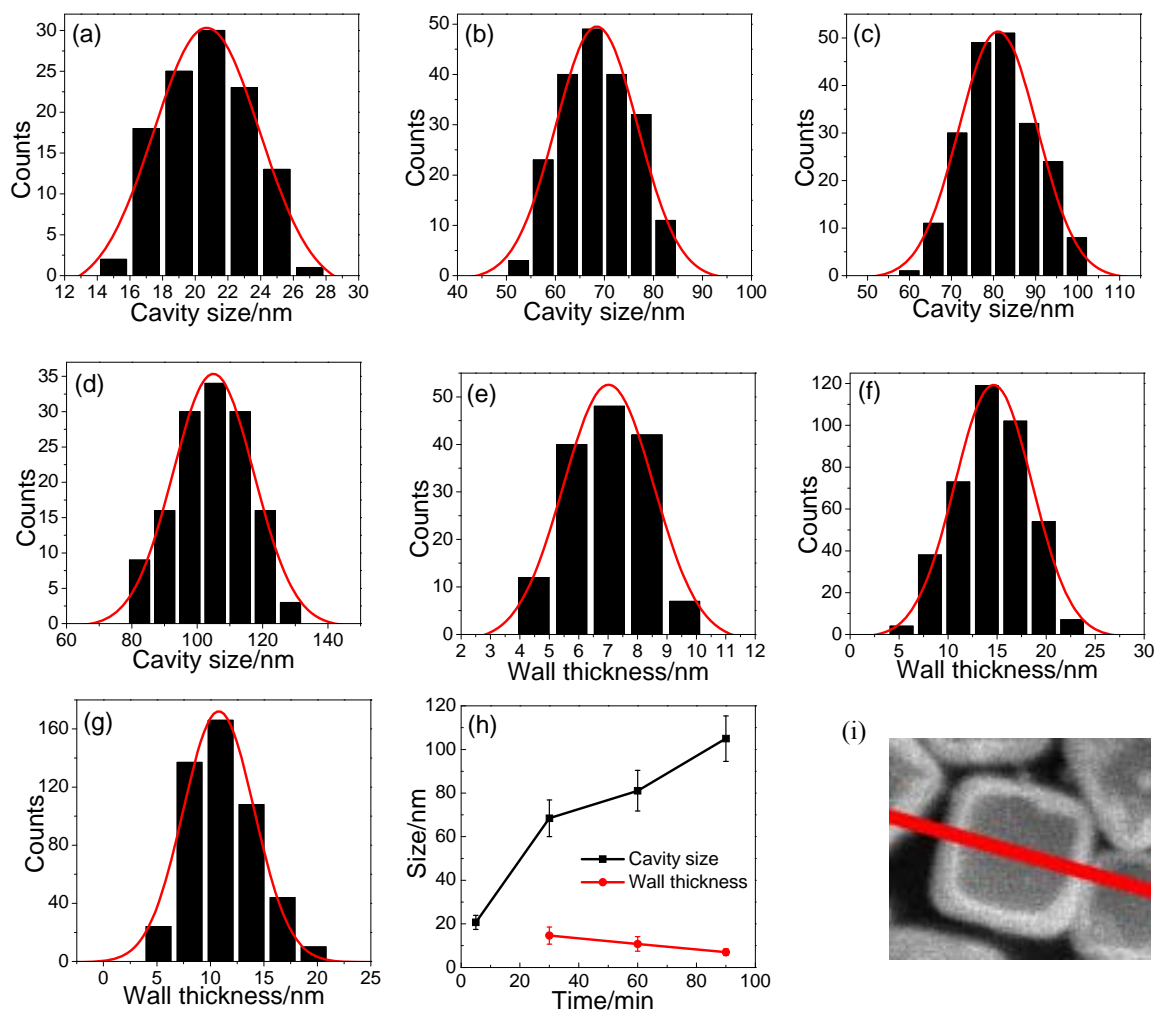


**Fig. S8** Distribution of cavity sizes (a-d) and wall thicknesses (e-g) of Ag nanocubes etched by different times: (a) 5 min, (b and e) 30 min, (c and f) 60 min, and (d and g) 90 min. (h) the correlation between cavity sizes/wall thicknesses and etching time. The measurement of cavity size was performed in the direction as marked with the red line in (i).

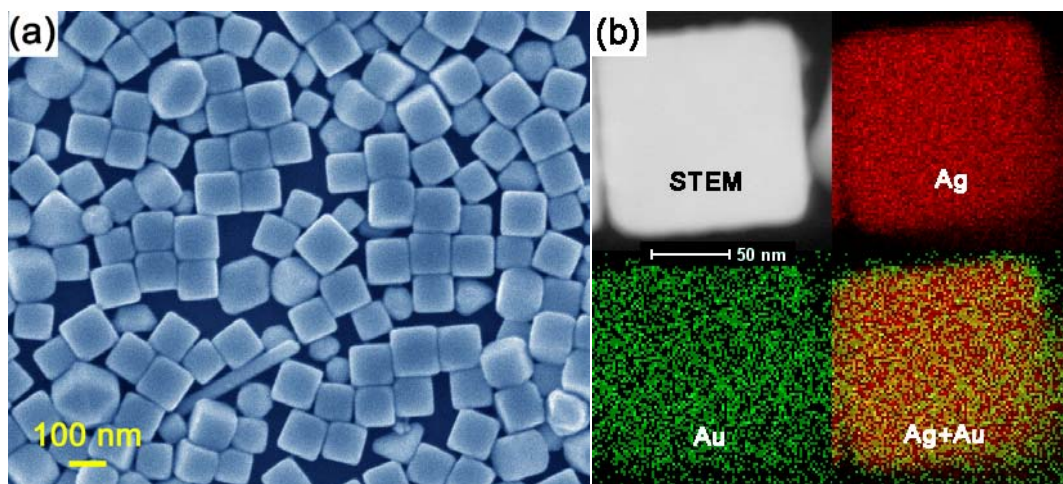


**Fig. S9** SEM (a) and STEM-EDX element mapping (b) image of Ag nanocubes located at water/toluene interface after addition of  $\text{AuCl}_4^-$  into the water for 4 h.

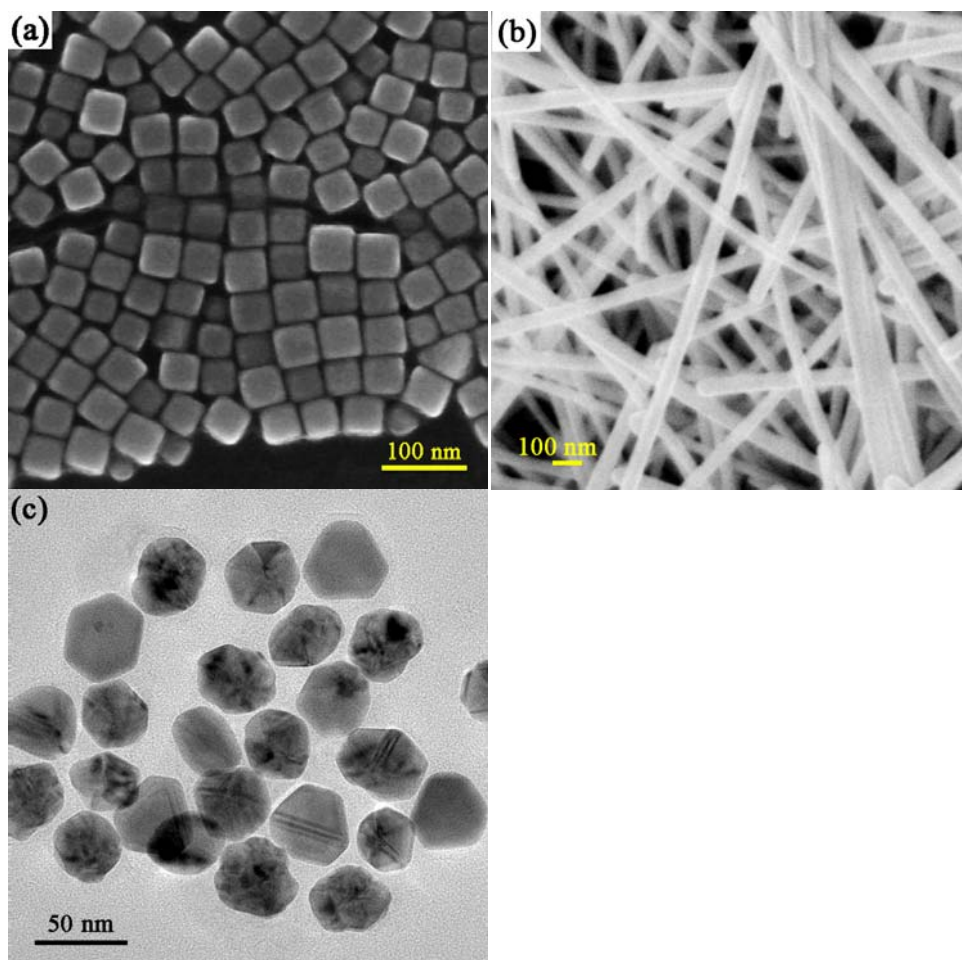


**Fig. S10** SEM images of  $\sim 45$ -nm Ag nanocubes (a), nanowires (b), and nanospheres (c).

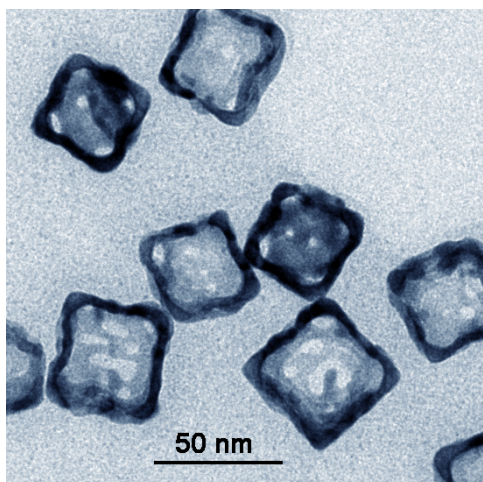


**Fig. S11** TEM image of  $\sim 45$ -nm Ag/Au nanocups with incomplete bottom layers obtained after etching for 30 min.

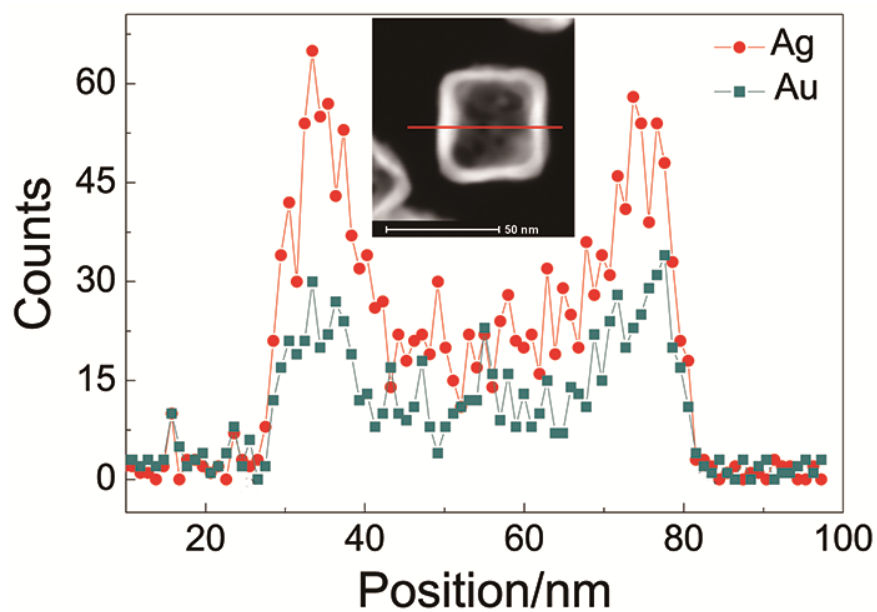


**Fig. S12** EDX linear scan element-distribution profile of Ag/Au nanocups obtained by etching ~45-nm Ag nanocubes for 30 min. Inset: the corresponding STEM image.



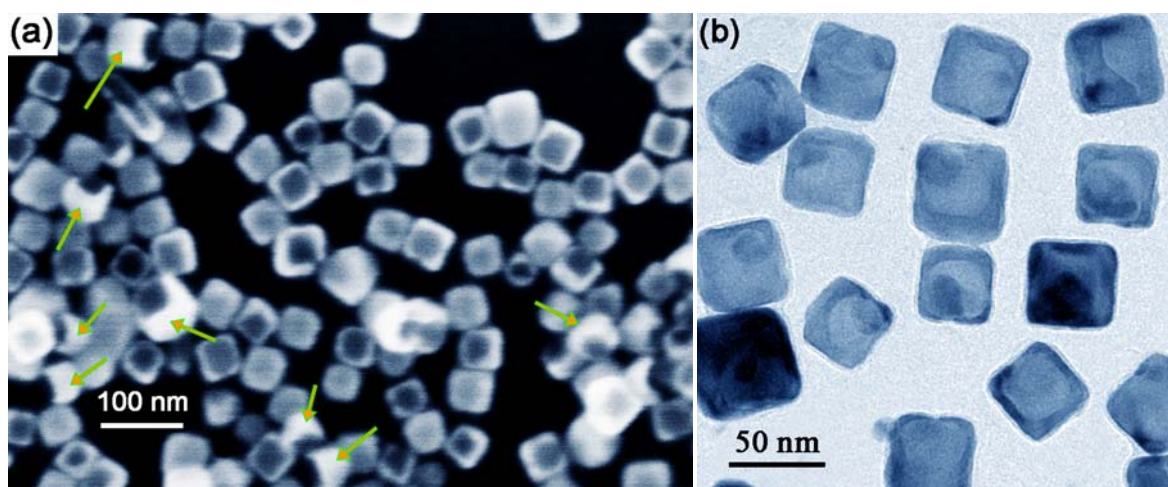


**Fig. S13** SEM (a) and TEM (b) images of  $\sim 45$ -nm Ag/Au nanocups obtained after etching for 10 min. Nanoparticles marked by arrows in (a) further demonstrate that etching occurs exclusively on the top face, and side faces are free of cavities. TEM image (b) shows that the bottom is closed. The resulting Ag/Au nanostructures are still nanocups.

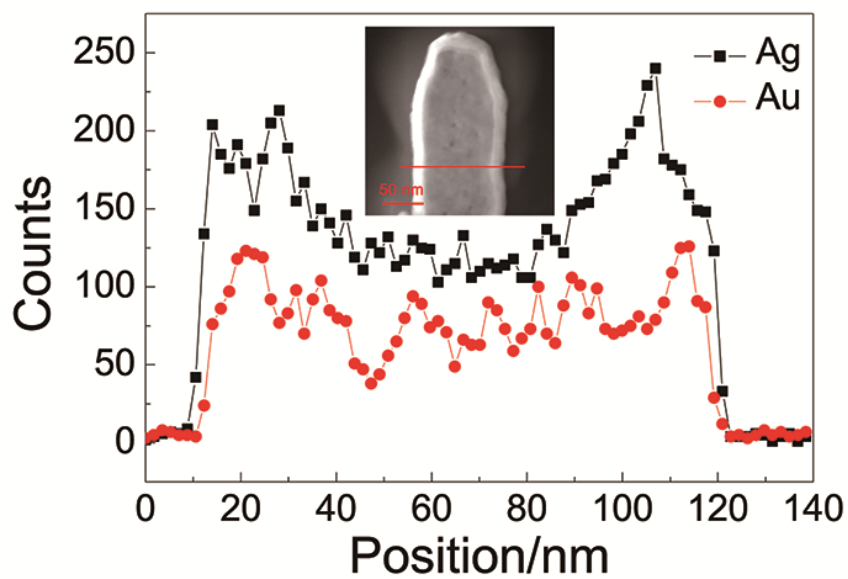


**Fig. S14** EDX linear scan element-distribution profile of Ag/Au nanocups obtained by etching Ag nanowires for 5 h. Inset: the corresponding STEM image.

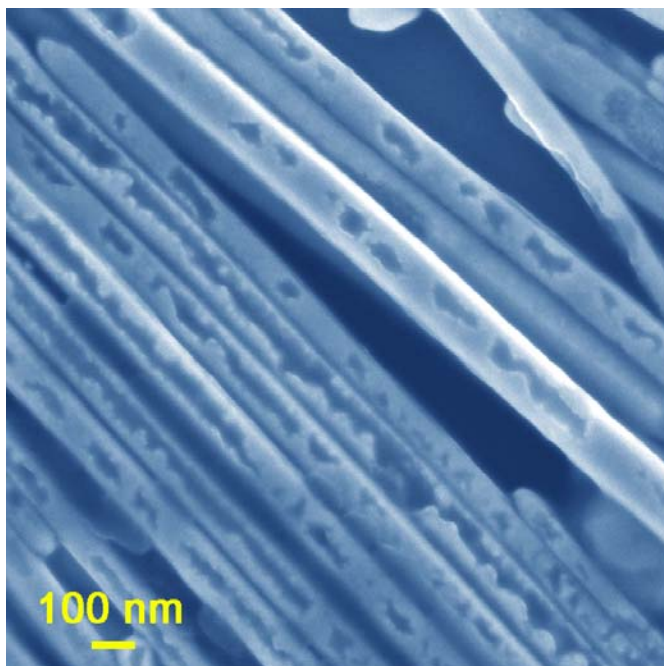


**Fig. S15** SEM image of Ag/Au nanowires with nanopits obtained by etching for 3 h.

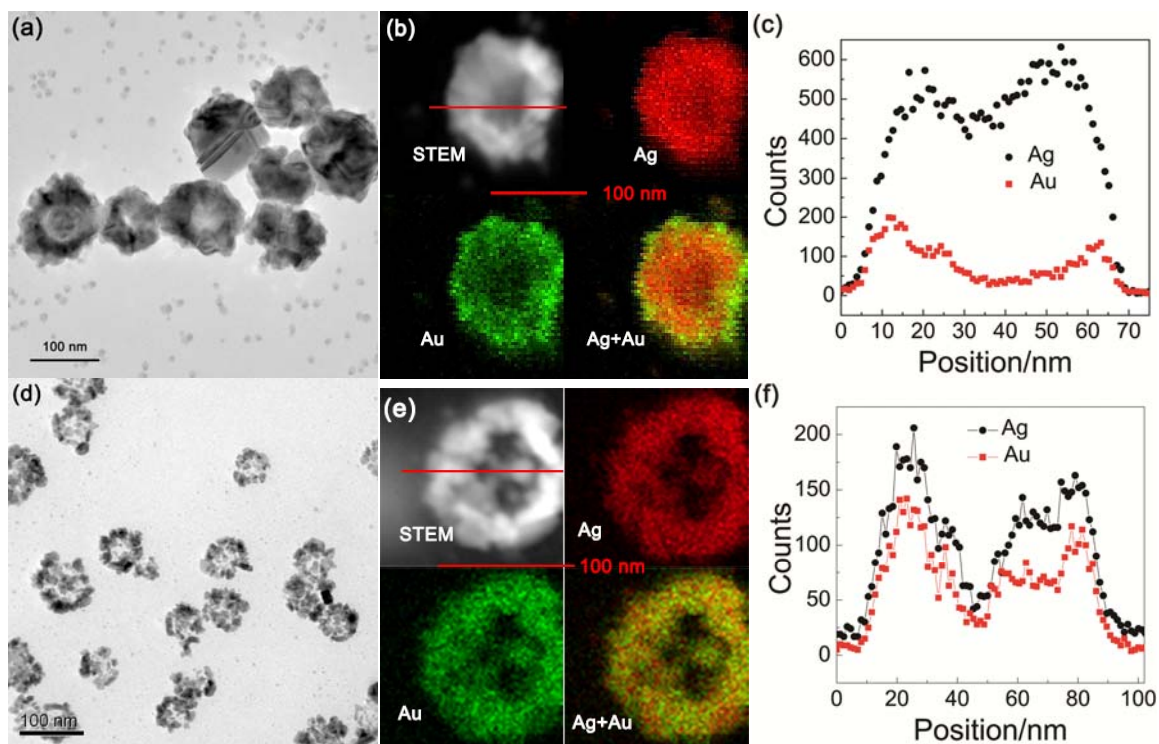


**Fig. S16** TEM (a and d), element mapping (b and e), and EDX linear scan element-distribution profiles (c and f) of Ag/Au spherical nanocups after etching different time: 5 min (a-c) and 30 min (d-e).

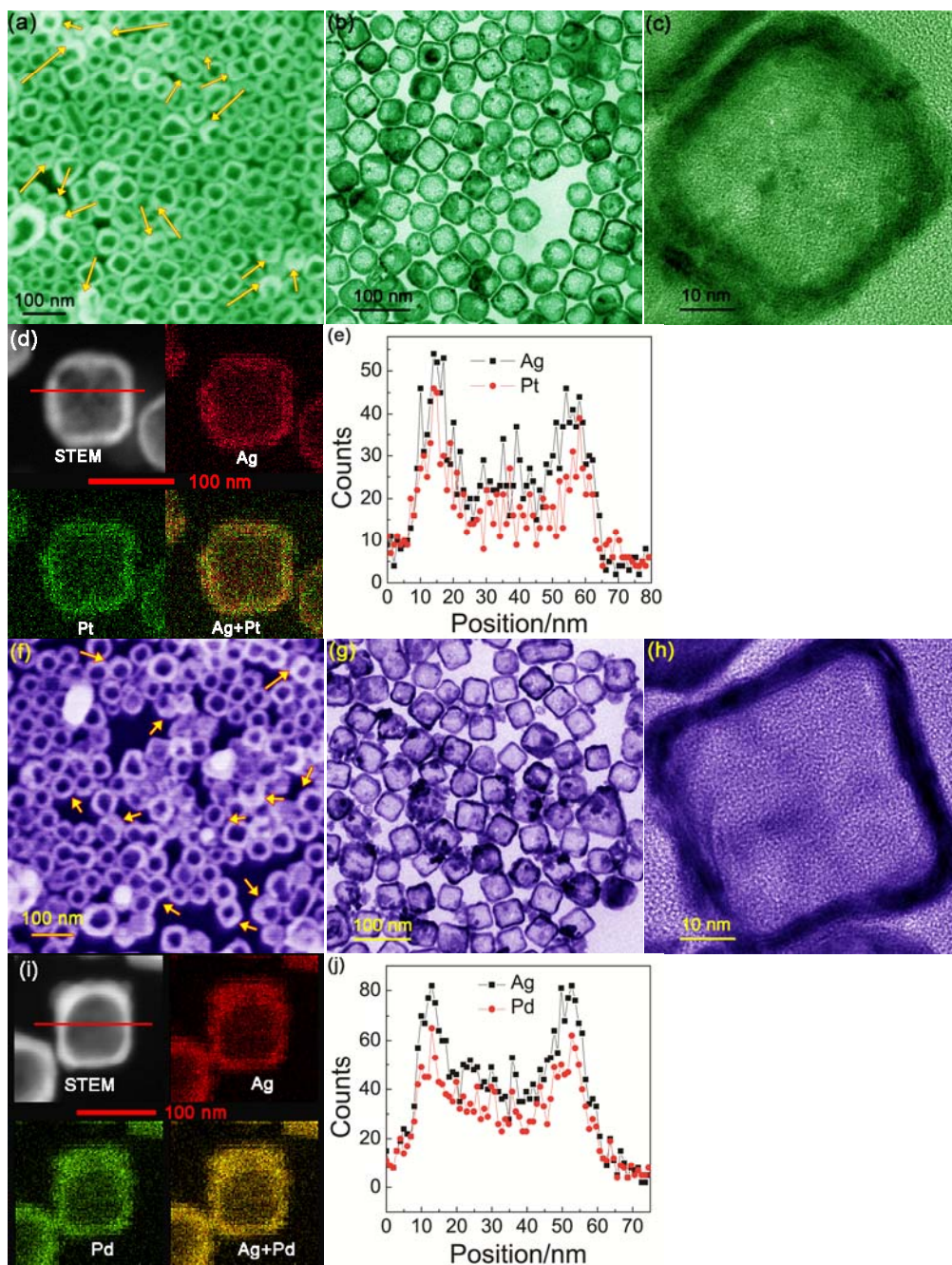


**Fig. S17** SEM (a and f), TEM (b and c; g and h), element mapping (d and i), and EDX linear scan element-distribution profiles (e and j) of Ag/Pt (a-e) and Ag/Pd (f-j) nanocups after etching for 45 min by  $\text{PtCl}_6^{2-}$  and  $\text{PdCl}_4^{2-}$ , respectively. Arrows marked in (a) and (f) shows that the resulting Ag/Pt and Ag/Pd nanostructures are still nanocups with walls free of cavities. The bottom thickness can be controlled by etching time. Compared with Ag/Au nanocups, Ag/Pt (d) and Ag/Pd (i) nanocups tends to alloy (d and i), especially for Ag/Pd nanocups.

## References

1. Tao, A.; Sinsersuksakul, P.; Yang, P. *Angew. Chem. Int. Ed.* **2006**, *45*, 4597.

2. Yang, Y.; Lee, Y. H.; Phang, I. Y.; Jiang, R.; Sim, H. Y. F.; Wang, J.; Yi, X. *Nano Lett.* **2016**, *16*, 3872.
3. Zhang, Q.; Cogley, C.; Au, L.; McKiernan, M.; Schwartz, A.; Wen, L.-P.; Chen, J.; Xia, Y. *ACS Appl. Mater. Interfaces* **2009**, *1*, 2044.
4. Shi, H.-Y.; Hu, B.; Yu, X.-C.; Zhao, R.-L.; Ren, X.-F.; Liu, S.-L.; Liu, J.-W.; Feng, M.; Xu, A.-W.; Yu, S.-H. *Adv. Funct. Mater.* **2010**, *20*, 958.
5. Bastús, N. G.; Merkoçi, F.; Piella, J.; Puentes, V. *Chem. Mater.* **2014**, *26*, 2836.
6. Liu, C.; Li, Y.-J.; Wang, M.-H.; He, Y.; Yeung, E. S. *Nanotechnology* **2009**, *20*, 065604.
7. Li, Y.-J.; Huang, W.-J.; Sun, S.-G. *Angew. Chem. Int. Ed.* **2006**, *45*, 2537.
8. Sun, Y.; Xia, Y. *Science* **2002**, *298*, 2176.
9. Moulder, J. F.; Stickle, W. F.; Sobol, P. E.; Bomben, K. D. *Handbook of X-Ray Photoelectron Spectroscopy*, Physical Electronics, Eden Prairie, MN, **1995**.